INTERNATIONAL JOURNAL OF
COASTAL, OFFSHORE & ENVIRONMENTAL ENGINEERING IJCOE Vol.8/No. 4/Winter 2023 (1-8)

Available online at: www. Ijcoe.org

Experimental Study on Assessing Interaction of Quay Walls and Random Waves Using Artificial Neural Network

Ramin Vafaeipour Sorkhabi[1*], Reza Gholi Ejlali[1], Alireza Naseri[1], Amin Hosseinchi Gharehaghaji [2]

[1] *Department of Civil Engineering, Tabriz Branch, Islamic Azad University, Tabriz, Iran*
[2] *Department of Geomatics Engineering, Faculty of Civil Engineering, University of Tabriz, Tabriz, Iran*

ARTICLE INFO

Article History:
Received: 18 Feb. 2020
Accepted: 11 Sep. 2023

Keywords:
Quay Wall
Random Waves
Strain
ANN
Peak Frequency
Wave Height

ABSTRACT

Quay walls are sheltering structures used for protecting coastal regions against wave-induced forces. Because of the random nature of the wave behavior, the application of physical models for the study of wave-structure interaction can be quite efficient. The aim of this study was to investigate the behavior of quay walls under random waves through experimental methods. The study used walls with vertical geometrical form, which were exposed to sea random waves under the JONSWAP spectrum. Surface level and wall strain values were measured using built-in sensors. A neural network model was developed using the feed-forward method with the backpropagation algorithm to analyze the time series of water surface level and strain. High coefficients of determination during the training and verification phases were observed, indicating good network performance. Self-correlation analysis of the time series showed that the data exhibited first-degree Markov characteristics. This finding was taken into consideration and increased the coefficients of determination in the neural network model.

1. Introduction

The wide coastlines in the country, the concentration of population and industry in the coastal areas, and damages from stormy waves necessitate examining the resistant structures against waves as one of the essential requirements [1]. Numerous studies have been conducted on the protection of coasts against waves. In a study, Alami et al. tested a combination of reinforced coastal structures to reduce wave energy and observed that with a decrease in wave height, coasts are subjected to less damage [2]. Quay walls are one of the most important structures, which significantly protect the coasts. In addition to bearing the sea waves that are imposed randomly, these walls should resist other forces such as earthquakes, sea currents, wind, and the impact of floats on the sea according to the environmental conditions. One of the important tools for measuring the interaction between these factors is the application of physical models used broadly by researchers and engineers in recent years [3]. The foundation of these models can be traced back to the 15th century when Leonardo DaVinci proposed the physical principles underlying them. Later in the 17th century, Newton provided a comprehensive explanation of these principles. To study such physical phenomena, it is essential to collect accurate data under controlled conditions. The collected data can then be processed and analyzed to gain insights into the problem. However, despite numerous studies on the reaction between quay walls and irregular waves, not many have explored the relationship between wave-induced forces and the internal forces acting on the walls. In this research, the wall strain was measured by identifying strain on the wall during interaction with the random wave. The relationship between them was specified via the experimental model [4]. The modeling of the neural networks between the wave forces and the wall strain determines the relationship between these parameters, and the appropriate coefficient of determination expresses the efficiency of this model. Sainflou proposed a method for determining the pressure resulting from irregular waves for the first time. The advantage of his method was the feasibility of its application. By this method, the pressure distribution can be estimated approximately in a direct line [5]. Rundgren (1958) showed that the Sainflou method depicts the random waves force more than the actual amount [6]. The Minikin theory was proposed in 1950 based on experimental observations on large

walls under regular broken waves. Indeed, the work of Mini Kane was the first experimental research that investigated the effect of Ashlee in his studies in a comprehensive way [7]. The most famous studies on the impact of the waves on the quay walls and vertical breakers were conducted by Goda in 2010 that are used by engineers for designing [8]. In experimental research, Vijayakrishna et al. (2004) investigated the dynamic wall response against regular waves in energy-absorbent structures [9]. Huge (2004) studied the flexural anchor in offshore structures against waves [10]. Nilamani et al. (2004) examined the impact of roughness on the quay walls as intrusion and extrusion chess blocks on the mentioned wall in an experimental approach and also studied the upstream and downstream waves and their effect on the implied forces by the waves. The wall was thin and deformable, and the back of the wall was considered vacant. The advantage of their work was using irregular waves and sloped walls with different slopes [11]. A method presented by Cumo et al. (2010) is suitable for scaling up impact pressures measured during small-scale physical model tests. The method accounts for air leakage's effect and applies to wave impact loads on different coastal structures. This methodology's applications to wave impacts on seawalls or caisson breakwaters have been studied [12].

Based on the conducted experimental and numerical studies, in the current research, the experimental study on assessing interaction of quay walls and random waves using ANN has been carried out using an artificial neural network.

2. Methodology

2.1. Random waves

In general, the waves are divided into regular and random waves. Random waves can be defined as a combination of regular waves. The sea waves in the stormy state are random [13]. In this condition, zero up Crossing and Zero down Crossing methods and the hydrodynamic wave features are mapped. The Zero up crossing method is common and used in this research. Figure 1 shows the Zero up crossing method [14, 15].

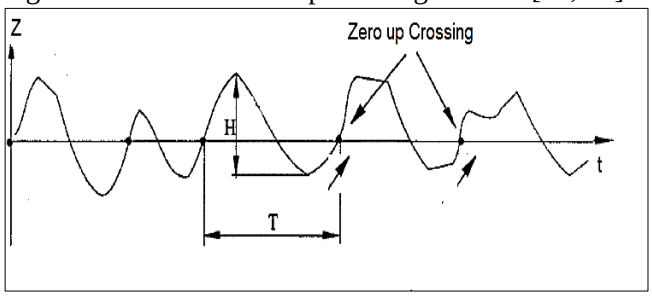

Figure 1. Random wave (field and experiential waves) [15]

2.2. Wave spectrum analysis

The random waves can be investigated using spectrum analysis on the recorded waves, which in this regard, spectrum density can offer a comprehensive justification of the waves in the sea conditions. Accordingly, the different spectrums, such as Bretschnider in 1959, P-M in 1964, TMA in 1985, and JONSWAP in 1974, were defined from the registered data. Sorenson introduced the JONSWAP spectrum as one of the most applicable spectrums in coastal structure design [16, 17]. A recent study has undertaken new research to create a spectrum that accurately reflects Iran's climate. To achieve this objective, the researchers utilized the JONSWAP spectrum, as depicted by Equation (1) and illustrated in Figure 2. These findings represent a significant step towards understanding and modeling Iran's climate patterns [14].

$$S(f) = \frac{\alpha g^2}{(2\pi)^4 f^5} e^{-1.25\left(f_p/f\right)^4} \gamma^a \quad (1)$$

Where γ is usually considered 1.6 to 6; however, 3.3 has been introduced as the best value in most references. The coefficient of γ is the density ratio in the maximum frequency spectrum JONSWAP to spectrum P-M [18]. Also, α and f_p Are defined in equations (2) to (4).

$$a = e^{-[(f-f_p)/(2\sigma^2 {f_p}^2)]} \quad (2)$$

$$\alpha = 0.076\left(\frac{gF}{W^2}\right)^{-0.22} \quad (3)$$

$$f_p = \frac{3.5g}{W}\left(\frac{gF}{W^2}\right)^{-0.33} \quad (4)$$

In these equations, *F*, Fetch length, *W* is the wind velocity, *f is the frequency, and* f_p is the peak frequency.

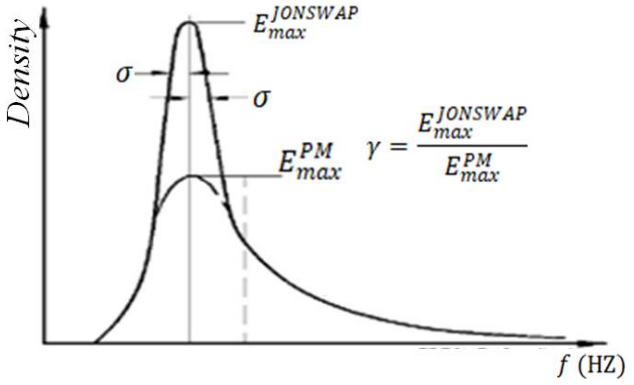

Figure 2. JONSWAP wave spectrum [19]

2.3. Physical model and experiments

The specifications were prepared for the current research, and the wave flume was designed and built in the Tabriz University Marine Structures Laboratory. The specifications used for experiments are as follows (figure 4).

- Length of flume: 12.5m
- Width of flume: 1.15m
-The length flume floor from the ground level is 75cm.
-Inside flume height: 1.05 m
- Water depth (d): 60 cm

-Wave generator type: hinged (Figure 3)
-Wall type: impermeable, without wave overhead, clipped on the floor, free in the margins
-Used waves: random under the JONSWAP spectrum
-Water level sampling frequency: 10 Hz
-Sampling frequency from the wall strain: 50 Hz

(a)

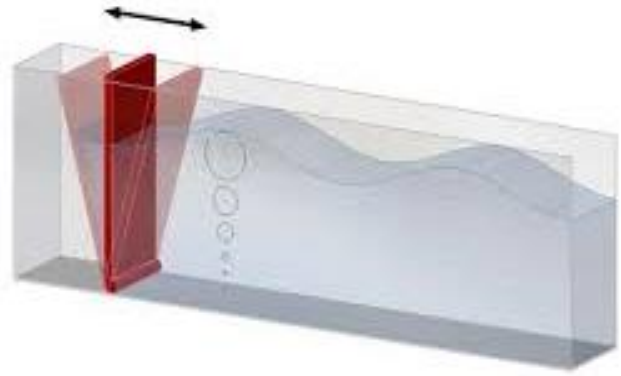

(b)

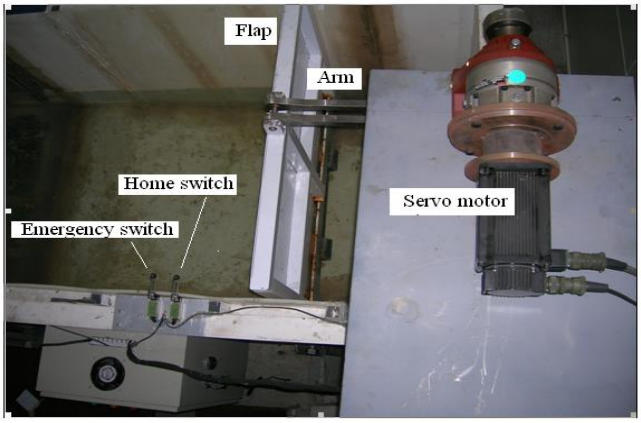

Figure 3. Hinged wave maker: (a) Schematic figure, (b) The hinged wave maker used in this research

Figure 4. Total view of the wave flume in the hydraulic laboratory

2.4. Generation and wave mapping

The JONSWAP spectrum input data is fed into the wave generator software via an input file, causing the paddle to initiate movement. However, as the numerical data may contain minor random fluctuations on the spectrum curve, generating these insignificant movements on the pedal is not feasible, and they must be eliminated. Consequently, a suitable filter is applied to the curve to remove any irregularities. The process of wave generation can be broken down into three simple steps, as illustrated in figures 5 and 6.

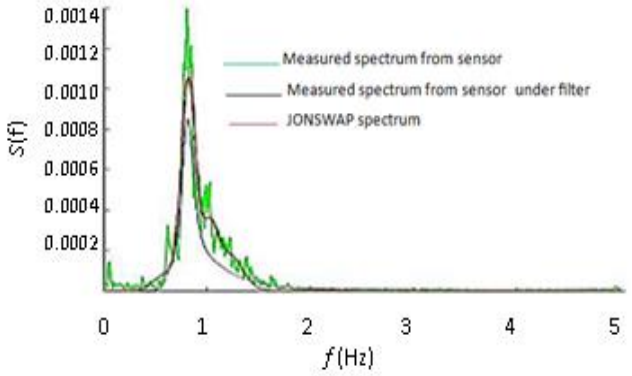

Figure 5. Primary spectrum (measured, filtered, and theoretic)

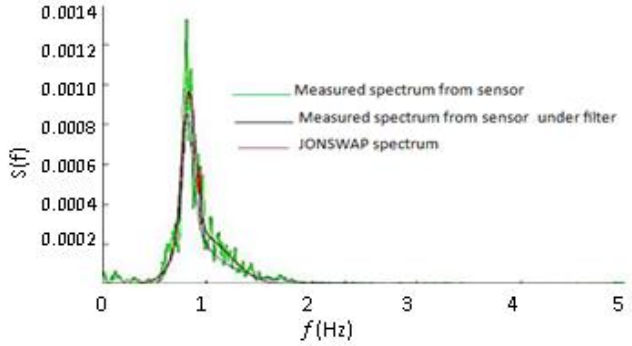

Figure 6. Modified spectrum (measured, filtered and theoretic)

-Generation of the primary wave based on the DSA numerical model and obtaining the spectrum resulting from the data mapped from sensor 1(MOD0).
-Modification of the obtained spectrum from step 1 according to the theoretic spectrum (MOD1).
-Repetition of step 2 in order to reduce the difference between the obtained spectrum and the theoretic spectrum (MOD2, 3).

2.5. Strain gauge

Strain gauges are TML Metal E-101R used for measuring flexural anchors as half-bridge. The sampling scope for the strain gauge varies from zero to 100Hz. Since the wall oscillation is faster than the water surface oscillation, thus it is necessary to pay attention to it in selecting the wall response sampling frequency to prevent the undesired problem of aliasing. In this research, the strain sampling frequency is 50Hz [20]. The manner of connection of the half-bridge and the details of the strain gauge are shown in Figure 7.

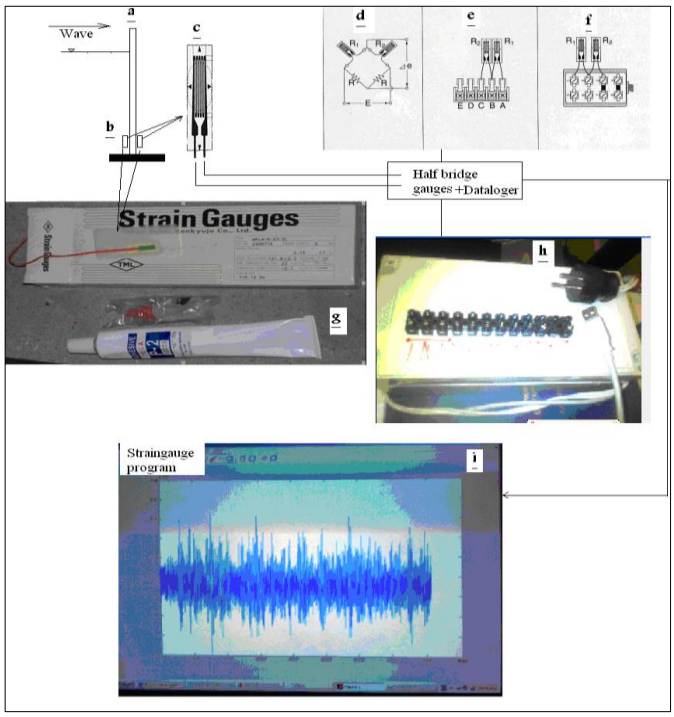

Figure 7. a) wall, b) place of the strain gauge on the wall, c) strain gauge schematic view, d) half-bridge connection to the unilateral data logger, e,f) strain gauge connection to the bilateral data logger, g) real image of strain gauge by special sticker, h) data logger, i) data images mapped from the strain gauge [20]

2.6. Experiments

Table 1 summarizes the experiments. The changes of the effective height are Hs from 3.9 to 9.2 cm, and peak frequency f_p ranges from 0.8 to 1.24 Hz. Table 1 presents the results of the five water level sensors used to measure fifteen waves in this study. For example, wave number 8 had a height of 5.4 cm and a peak frequency of 1.2 Hz at the water surface level, as indicated in the table. In this table H_s is significant wave height. To ensure accurate water level measurements in each experiment, mapping was performed from the still water surface and saved in separate files as time series data. Concurrently, strain gauges were installed on the wall to determine the pure strain caused by each wave. Consequently, for wave number 8, Table 3 and the strain gauge results corresponding to Table 2 were proposed. As the strain gauge was only installed on the wall, a time series file was created for strain measurements.

The wave absorber at the end of the channel is a metal mesh plate designed to absorb wave energy and prevent wave reflection. By absorbing the wave energy, it effectively eliminates the return wave and wave reflection.

Table 1. specifications generated random waves by JONSWAP spectrum based on the wave effective height and peak frequency

Number of Tests	H_s (cm)	Peak Frequency
1	5	0.8
2	5.2	1.24
3	5	1
4	5.6	1.23
5	7.3	1.22
6	3.9	1.23
7	5.4	1
8	5.4	1.2
9	4.3	1.23
10	7.7	1.21
11	6	1.23
12	7.5	1.23
13	9.2	1.23
14	5.6	1.24
15	7.5	1.21

Table 2. mappings for determining the wave from the water surface level sensors

Sensor	Water Surface Level	Water Static Surface Level
WP1 sensor	W1	W001
WP2 sensor	W2	W002
WP3 sensor	W3	W003
WP4 sensor	W4	W004
WP5 sensor	W5	W005

Table 3. mappings for determining the strain from the strain gauge built on the wall

Sensor	Strain File Name	The Strain File Name for Wall Still State
SG1	E1	E

2.7. Artificial neural networks modeling

Artificial neural networks have become increasingly prevalent in various fields, including engineering. In hydraulic engineering, the backpropagation algorithm is commonly utilized. Recent research has demonstrated that using a three-layer backpropagation algorithm can yield promising outcomes for prediction and simulation purposes in this field [21]. In this section, the neural network modeling was done based on the time series mapped from the experiments. Based on the research, the interaction between the wall and random waves is being studied. In this context, the water level time series are considered as input data, while the strain time series is considered as output data. The purpose is to analyze and understand the relationship between the wall and the waves, with a focus on measuring the strain and pressure exerted by the waves on the wall. Hence, changes in the water surface level can investigate the strain and pressure changes.

2.8. Network structure

Figure 7 depicts the feed-forward neural network with a backpropagation algorithm. This structure has been used in predicting the engineering works time series and is employed in this research. Based on this structure, nonlinear mapping is done between the input and output values. The feed-forward method is achieved based on the linear combination of the input

values leading to a nonlinear function. In Figure 8, i is related to the input layer, % is associated with the middle layer, j relates to neurons output, and k is the weight of the neurons in the feed-forward method, the connection among the neurons is done only by the middle layer. Equation (5) depicts the network output.

$$\hat{y}_k = f_0\left[\sum_{j=1}^{M} w_{kj}.f\left(\sum_{i=1}^{N} w_{ji}.x_i\right) + w_{j0}\right] \quad (5)$$

Where w_{ji} is the middle layer between neuron i from the input layer and neuron j from the middle layer, w_{j0} is the bios of neuron j , and f_h is the actuator function of the middle layer, w_{kj} is the output layer weight between neuron k from the output layer and j from the middle layer, f_0 is the actuator function for the output neuron, x_i is the input value in the input layer, $\hat{y}$ and y are the calculative and observation output values. The weights values differ in the middle and output layers and change in the network phase. The selective actuator functions are sigmoid logarithmic. The time series used in neural networks are normalized. Since these experimental data are related to some waves, they will be as positive and negative. Thus, this issue should be considered in their normalization. In the chapter on the analysis of the normalized form, the division of the time series was used as the maximum absolute value of the data in the time series. The data are used in this section based on this normalized method. On the other hand, applying this method is simple and common in engineering works [21].

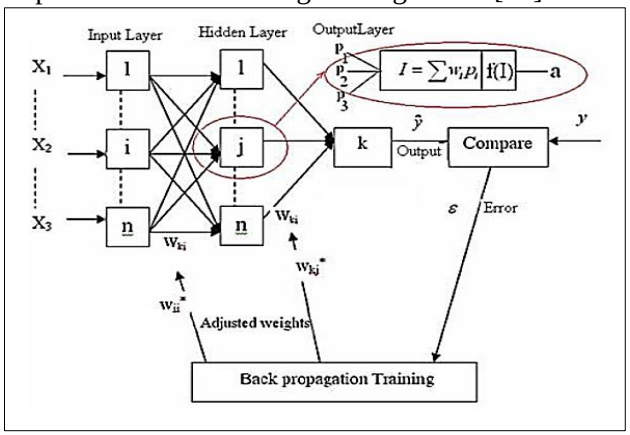

Figure 8. feed-forward neural network structure with the backpropagation algorithm with three layers [21]

2.9. Neural networks model

Various techniques are available for training and validating neural networks. A widely adopted approach for validation involves selecting one-third of the input and output time series from the beginning and one-third from the end [21]. The training process involves creating a model, and based on the model, the validation is predicted. To assess the quality of the network, regression coefficients are calculated for both the training and validation phases. The coefficient of determination, as expressed in equation (6), indicates how well the model performs, with a value closer to one indicating better performance. The Root Mean Square Error coefficient, as expressed in equation (7), is another metric used to evaluate model performance, with values closer to zero indicating superior performance.

$$R^2 = 1 - \frac{\sum_{i=1}^{N}(E_i - \hat{E}_i)^2}{\sum_{i=1}^{N}(\hat{E}_i - \overline{E})^2} \quad (6)$$

$$RMSE = \sqrt{\frac{\sum_{i=1}^{N}(E_i - \hat{E}_i)^2}{N}} \quad (7)$$

R^2, $RMSE$, N, E_i and $\overline{E}$ are coefficient of determination Root Mean Square Error, number of observations, strains obtained in the experiment (prediction values), and the average of strains related to the strain time series [22].

3. Results and discussion

If the time series of the water surface level is shown with W_t and the strain time series is depicted by E_t, the third-fourth W_t is considered as the training input from the beginning and one-fourth W_t, as verification input from the end, and one-fourth E_t as verification output from the end. Table 4 summarizes the values of the coefficient of determination in the training section (R_t^2) and verification (R_v^2) based on the network architecture. The network architecture inserts the input, middle, and output neurons. For instance, the (2-1-3) is meant the number of input neurons 2, central neuron 1 and output neuron 3. As is seen from Table 4, after 200 repetitions with network architecture of (1-5-1), the coefficients of determination are constant. Thus, R_t^2=0.7699, R_t^2=0.7743 are considered as coefficients.

Table 4. Results of BP-FFNN model in prediction of the water surface level strain

ANN architecture	epoch	R_v^2 (Calibration)	R_t^2 (Training)
1-2-1	50	0.7683	0.7681
1-2-1	100	0.7686	0.7688
1-2-1	150	0.7686	0.7701
1-2-1	200	0.7690	0.7710
1-2-1	250	0.7690	0.7710
1-2-1	300	0.7690	0.7710
1-2-1	400	0.7690	0.7710
1-2-1	500	0.7690	0.7710
1-3-1	200	0.7692	0.7713
1-4-1	200	0.7695	0.7731
1-5-1	**200**	**0.7699**	**0.7743**
1-6-1	200	0.7699	0.7743
1-7-1	200	0.7699	0.7743
1-5-1	300	0.7699	0.7743

Figure 9 shows the experimental and calculation results of water surface level strain prediction of the neural network model. Figure 9 depicts the regression curve for training, verification, and water surface level strain prediction. The obtained conversion coefficients for

training and verification depict better performance of the neural network models.

Figure 9 shows the experimental and calculation results of water surface level strain prediction of the neural network model.

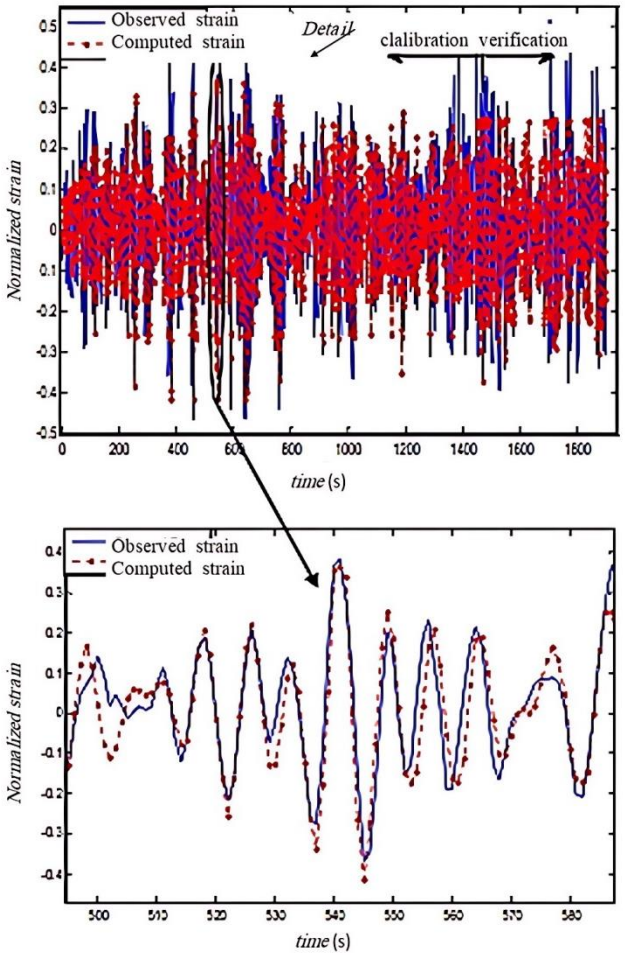

Figure 9. experimental and calculation results of strain prediction

Figure 10 depicts the regression curve for training, verification, and predicting water surface level strain. The obtained conversion coefficients for training and verification depict better performance of the neural network models. If there is a linear curve between time series y_t and the same time series with a step backward y_{t-1}, the first-grade self-correlation is established, and if there is a linear curve between y_t, and y_{t-2}, the second-grade self-correlation is established, and this trend is continued if the inputs x_t, and output y_t, are assumed, according to the Markov chain of rules, can be used for the prediction of the time series of first-grade Markov y_t, $X_t = \begin{bmatrix} x_t \\ y_{t-1} \end{bmatrix}$ and for second grade Markov $y_t, X_t = \begin{bmatrix} x_t \\ y_{t-1} \\ y_{t-2} \end{bmatrix}$ that provide better results relative to $X_t = [x_t]$. Because the behavior is not completely linear, all cases are usually considered in prediction. In Figure 11, the curve between E_t and E_{t-1} has been drawn and $R^2 = 0.5998$ was achieved, and Figure 12 shows $R^2 = 0.0122$ between E_t and E_{t-2}. Thus, the date on the strain time series is first-grade Markov.

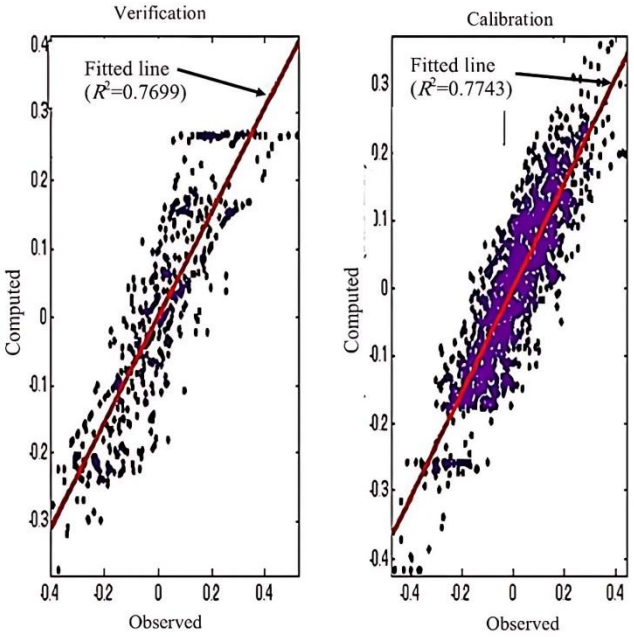

Figure 10. regression curve for training, verification, and water surface level strain prediction

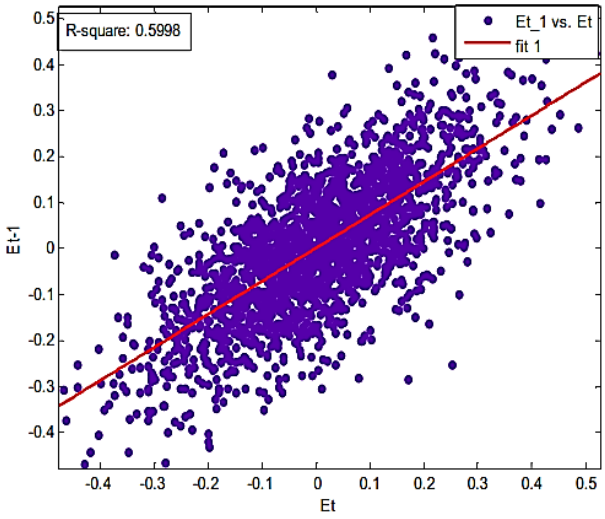

Figure 11. linear regression between E_t and E_{t-1}

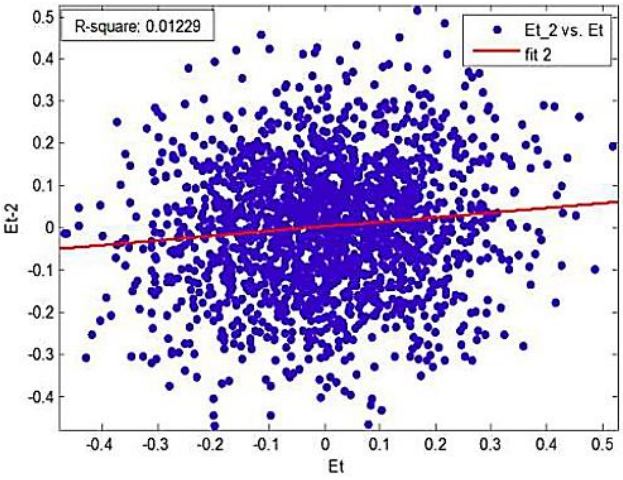

Figure 12. linear regression between E_t and E_{t-2}

The results of the neural network model are shown according to Table 5, considering first and second-grade Markov equations for strain and pressure. In these tables, it is seen that the value of R2 is increased by considering the first-grade Markov. On the other hand, in the case that $\begin{bmatrix} W_t \\ E_{t-1} \end{bmatrix}$ is considered in determining input strain instead of [W_t], the value of R^2 increases from 0.7773 to 0.8109.

Table 5. Results obtained from BP-FFNN model in prediction of strain from water surface level

Input	Output	ANN architecture	epoch	R_v^2 (Calibration)	R_t^2 (Training)
$[W_t]$	E_t	1-5-1	200	0.7699	0.7743
$\begin{bmatrix} W_t \\ E_{t-1} \end{bmatrix}$	E_t	**2-8-1**	**250**	**0.8418**	**0.8109**
$\begin{bmatrix} W_t \\ E_{t-1} \\ E_{t-2} \end{bmatrix}$	E_t	3-9-1	250	0.6536	0.6395

4- Conclusion

The present study aimed to investigate the behavior of quay walls under the influence of random waves, using experimental methods. Vertical geometrical form walls were exposed to sea waves with JONSWAP spectrum, and their surface level and wall strain values were measured using built-in sensors. The study utilized a neural network model, which employed the feed-forward method with the backpropagation algorithm. The model used time series data of water surface levels and strains to predict their behavior. Finally, the following results can be mentioned:

- The results of the study showed that the high conversion coefficients in the training and verification phases of the artificial neural networks modeling indicate better network performance.

The BP-FFNN model was able to predict the water surface level strain, and the best ANN architecture was (1-5-1), with epoch 200 and coefficients of determination Calibration and Training of 0.7743 and 0.7699, respectively, which are acceptable coefficients.

- The data on the series showed first-grade self-correlation (first-grade Markov) between water surface level and wall strain.
- The best ANN architecture was (2-8-1), with epoch 250 and coefficients of determination Calibration and Training of 0.8418 and 0.8109, respectively. Moreover, the first-grade Markov performed better than higher grades of Markov.

5. References

[1] Vafaeipour Sorkhabi, R., Naseri, A., Alami, M. T., and Mojtahedi, A. (2022), *Experimental Study of an Innovative Method to Reduce the Damage of Reshaping Rubble Mound Breakwaters*, Innovative Infrastructure Solutions, 7(6), 353.

[2] Alami, M. T., Vafaeipour Sorkhabi, R., Naseri, A., and Mojtahedi, A. (2022), *Enhancing Stability and Reduce Damage in Rubble-Mound Reshaping Breakwaters by Using Obstacles in Front of the Structure*, Civil Infrastructure Researches, 7(2), 33-49.

[3] Vafaeipour Sorkhabi, R., and Naseri, A. (2021), *Experimental Investigation of Optimal Slope Determination of Seawalls Subjected to Random Sea Waves based on Base Shear and Overturning Moment*, Amphibious Science and Technology, 2(3), 37-49.

[4] Vafaeipour Sorkhabi, R., and Naseri, A. (2019), *Experimental Investigation of the Interaction Between Vertical Flexible Seawall and Random Sea Waves*, Journal of Advanced Defense Science & Technology, 6(3): 155-162.

[5] Sainflou, G., (1928), *Essai sur les digues maritimes verticals*. Annales de ponts et chaussées, 98(1), 5-48.

[6] Rundgren, L., (1958), *Water wave forces : a theoretical and laboratory study*, Bulletin 549 Royal Institute of Technology, Division of Hydraulics, Stockholm, Sweden.

[7] Minikin, R., (1950), *Wind Waves and Maritime Structures: Studies in Harbor Making and in Protection of Coasts*, Charles Griffin & Company, London, 224-304.

[8] Goda, Y., (2010), *Random Seas and Design of Maritime Structures*, Advanced Series on Ocean Engineering, World Scientific.

[9] Vijayakrishna, E., Natarajan, and R., Neelamani, S., (2004), *Experimental Investigation on the Dynamic Response of a Moored Wave Energy Device under Regular Sea Waves*, Ocean Engineering, 31(5): 725- 743.

[10] Hughes, S.A., (2004), *Wave momentum flux parameter: A Descriptor for Near Shore Waves*, Coastal Engineering, 51(11): 1067-1084.

[11] Neelamani, S., Jawguei, L., and Shangchun, C., (2010), *An Experimental Study of Wave Forces on Vertical Breakwater*, Journal of Marine Science and Technology, 15(3): 158-170.

[12] Cumo, G., Allsop, W., and Takahashi, S., (2010), *Scaling Wave Impact Pressures on Vertical Wall*, Coastal Engineering, 57 (6): 604-609.

[13] Vafaeipour Sorkhabi, R., Alami, M., Naseri, A., and Mojtahedi, A. (2022), *Experimental Analysis of the Effect of a Submerged obstacle and Floating Wave Barrier in front of a Rubble Mound Breakwater on Diminishing the Damage Parameter*, International Journal of Coastal, Offshore and Environmental Engineering, 7(2), 39-48.

[14] SPM, (1984), *Shore protection manual*, Coastal Engineer's Research Center, U.S Army corps.

[15] Osgouei, A. D., Poursorkhabi, R. V., Maleki, A., and Ahmadi, H. (2021), *Effects of a Floating Wave*

Barrier with Square Cross Section on the Wave-induced Forces Exerted to an Offshore Jacket Structure, Ocean Systems Engineering, 11(3), 259-274.

[16] Naseri, A., Sorkhabi, R. V., Alami, M. T., and Mojtahedi, A. (2022), *Damage Parameter Variations of Breakwater along with a Floating Wave Barrier and a Submerged Obstacle*, International Journal of Sustainable Construction Engineering and Technology, 13(1), 202-217.

[17] Vafaeipour, R., Lotfollahi, M., and Aminfar, M., (2011), *The Effect of Random Waves Period on Coastal Wall Reaction with Various Geometrical Shapes with Numerical Method*, Journal of Oceanography, 8, 69-78.

[18] Sorensen, R.M., (1993), *Basic Wave Mechanic for Coastal and Ocean engineering*, Jon Wiley.

[19] Alami, M., Vafaeipoor, R., Naseri, A., Mojtahedi, A. (2022), *Experimental Analysis of the Effect of the Distance of a Submerged Berm in front of a Reshaping Rubble Mound Breakwater on Diminishing the Damage Parameter*, Journal of Civil and Environmental Engineering, 52.2(107), 1-13.

[20] Strain Gauge TML Pam E-101R, (2012), Sokki Kenkyujo Company, Ltd. Tokyo.

[21] Nourani, V., komasi, M., and Mano, A., (2009), *A Multivariate ANN - Wavelet Approach for Rainfall Runoff Modeling*, Water Recourse Management, 36,1251-1257.

[22] Motamedi, H., Rahbani, M., Harifi, A., and Ghaderi, D. (2020). *The choice between Radial Basis function and Feed Forward Neural Network to predict long term tidal condition.* International Journal of Coastal, Offshore And Environmental Engineering, 5(1), 1-9.